

Yusuke Taniguchi · Kosei Ando

Time dependence of Poisson's effect in wood I: the lateral strain behavior

Received: May 15, 2009 / Accepted: August 7, 2009 / Published online: November 21, 2009

Abstract To understand the viscoelasticity of wood three dimensionally, a longitudinal tensile creep test for 12 species was conducted to examine the changes with time in the lateral strain and the viscoelastic, i.e., apparent Poisson's ratio. The changes in the lateral strain (ε_T and ε_R) were similar to those in the longitudinal strain (ε_L). That is, during creep, the absolute value of lateral strain continued to increase with the gradual reduction in the increase rate; immediately after the removal of the load, it recovered abruptly; then, it recovered slowly and finally reached a certain value. The rate of increase in the longitudinal strain during creep was smaller than that in the absolute value of lateral strains. The apparent Poisson's ratio became large during creep because the lateral strain increased more than the longitudinal strain. The analysis of lateral strain by decomposition into three components, that is, instantaneous strain, delayed elastic strain, and permanent strain, has revealed that the lateral permanent strain in the transverse direction contributes most to the increase in the apparent Poisson's ratio during creep.

Key words Creep · Poisson's ratio · Viscoelasticity · Lateral strain · Permanent strain

Introduction

Because wood is frequently used as the structural component of buildings, furniture, etc., the study of its viscoelastic properties, such as creep and stress relaxation, is important.

Y. Taniguchi · K. Ando (✉)
Graduate School of Bioagricultural Sciences, Nagoya University,
Chikusa-ku, Nagoya 464-8601, Japan
Tel. +81-52-789-4149; Fax +81-52-789-4147
e-mail: musica@agr.nagoya-u.ac.jp

Part of this article was presented at the 18th meeting of the Chubu Branch of the Japan Wood Research Society, Ogaki, Japan, November 13, 2008

The longitudinal strain that occurs during creep is a parameter crucial for structural maintenance, and therefore many papers have discussed this subject.^{1,2} However, the lateral strain behavior resulting from Poisson's effect has hardly been discussed, despite its importance for the three-dimensional understanding of wood's viscoelasticity and for its long-term dimensional stability.

Poisson's ratio is an indicator of Poisson's effect.^{3–5} Wood has three orthotropic axes: longitudinal (L), radial (R), and tangential (T). In such an anisotropic system, six Poisson's ratios are required to describe the three-dimensional elasticity. The ratio of passive to active strain is defined as Poisson's ratio, ν_{ij} :

$$\nu_{ij} = \left| \frac{\varepsilon_j}{\varepsilon_i} \right| \quad (1)$$

where i refers to the direction of longitudinal strain and j to lateral strain. Concerning orthotropism, Poisson's ratios of wood have been measured.^{6–9} According to Jeong et al.,¹⁰ Poisson's ratio of loblolly pine was significantly different for different growth rings and intra-ring layers (earlywood and latewood). Yadama et al.¹¹ indicated that Poisson's ratio of aspen became relatively small with increasing fiber angle. Peura et al.^{12,13} determined the Poisson's ratio for crystalline cellulose in Norway spruce by tensile testing with in situ X-ray diffraction.

It is known that Poisson's ratio in wood has a weaker correlation with the wood's strength properties (compressive strength, tensile strength, and shearing strength) than other elastic constants such as Young's modulus and the shear modulus.¹⁴ Also, it appears that no common explanation has been given regarding the density dependence¹⁵ because of the excessive scattering of the data obtained. In addition, Poisson's ratio in wood exhibits a peculiar dependence on moisture content,¹⁶ that is, ν_{LT} , ν_{TL} , ν_{RT} , and ν_{TR} increase linearly with the increase in moisture content, whereas ν_{LR} and ν_{RL} decrease with the increase in moisture content. This peculiarity of Poisson's ratio in wood suggests that the mechanism of Poisson's effect in wood is greatly dominated by the microscopic/macroscopic tissue structure

of wood. Morooka et al.¹⁷ and Ohgama¹⁸ have shown that the porous structure of wood affects mainly the Poisson's ratios (ν_{RT} , ν_{TR}), according to the results of numerical analysis using a model.

Some reports concerning Poisson's ratio are available to resolve the two- or three-dimensional viscoelasticity of wood. Hilton et al.^{19,20} investigated anisotropic and isotropic Poisson's ratio time effects analytically and evaluated numerically. They proved that "real" viscoelastic material has a time-dependency entirely of viscoelastic Poisson's ratios and demonstrated the close relationship between viscoelastic moduli and Poisson's ratios. Taniguchi et al.²¹ measured the changes with time in the viscoelastic, i.e., apparent Poisson's ratio of Japanese cypress, to determine the three-dimensional viscoelastic compliance tensor.

In this study, we examined the lateral strain behavior of 12 species by conducting longitudinal tensile creep tests with the aim of understanding the viscoelasticity of wood three dimensionally. In our study, we defined the absolute value of the lateral strain divided by the longitudinal strain, measured during creep and creep-recovery, as the apparent Poisson's ratio, to use it as an indicator for evaluating the Poisson's effect quantitatively.

Materials and methods

Materials

Regarding the species, Japanese beech (*Fagus crenata*), Japanese ash (*Fraxinus mandshurica*), Japanese zelkova

(*Zelkova serrata*), Japanese chestnut (*Castanea crenata*), teak (*Tectona grandis*), and balsa (*Ochroma lagopus*) were used as the hardwoods, and Japanese cedar (*Cryptomeria japonica*), Japanese cypress (*Chamaecyparis obtusa*), ezo spruce (*Picea jezoensis*), genus *Agathis* (*Agathis* sp.), Douglas-fir (*Pseudotsuga menziesii*), and western red cedar (*Thuja plicata*) were used as the coniferous woods. Table 1 shows the density and moisture content of 12 species.

Figure 1 shows an overview of a tensile test specimen. The specimen measured 300 mm along the fiber, 17.5 mm radially, and 17.5 mm tangentially. A tapered shape with a central cross section of 12 mm \times 12 mm and a parallel portion of about 30 mm along the fiber was formed on the LT and LR planes. To the grip sections on both ends of the specimen, tabs made of a hardwood were adhered for reinforcement. Specimens were conditioned to equilibrate a moisture content at a constant 25°C and 55% relative humidity over a period of 3 months.

Tensile creep test

For the tensile test, a servo-controlled fatigue-testing machine (Shimadzu Servopulser EHF-ED10/TD1-20L) was used. The biaxial strain gauges (gauge length, 2 mm; Tokyo Sokki Kenkyujo, FCA-2-11) were pasted to the respective center parts on the opposite LT and LR planes (four planes) of the specimen to measure the longitudinal strain (ϵ_L) and lateral strains (ϵ_T , ϵ_R) serially.

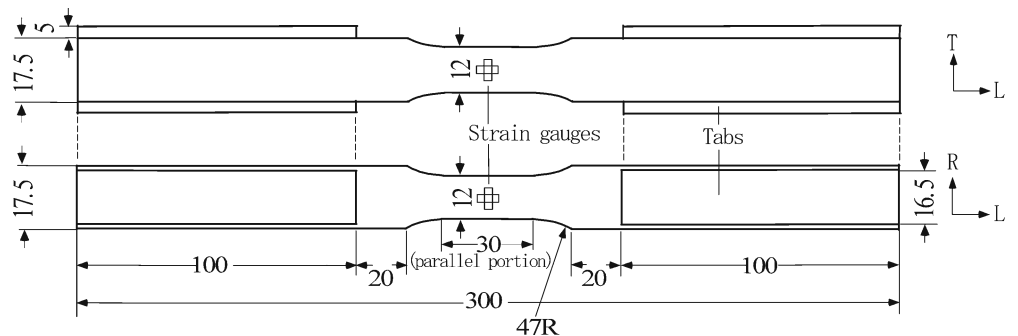
Beforehand, a static tensile test was conducted with a loading speed of 98 N/s to measure the tensile strength. All

Table 1. Mean values of density, moisture content, and applied stress in 12 species for the creep test

Species	Density (kg/m ³)	Moisture content (%)	Applied stress (MPa)	<i>n</i>
Japanese cypress	411	9.6	67	2
Japanese cedar	367	9.8	55	2
Ezo spruce	338	10.0	56	2
Genus <i>Agathis</i>	472	9.8	76	3
Douglas-fir	457	9.3	63	3
Western redcedar	457	10.2	56	4
Japanese beech	572	9.9	69	3
Japanese ash	557	9.5	61	2
Japanese zelkova	630	10.4	60	2
Japanese chestnut	584	9.6	63	2
Teak	684	9.8	82	3
Balsa	110	9.0	9.5	1

Applied stress is equal to 50% of tensile strength
n, Number of specimens

Fig. 1. Tensile test specimen. Biaxial strain gauges were pasted on the four planes. Unit, mm



the specimens for static and creep tests were prepared from the same lumber for each species. More than five specimens were used for the static test for each species. A specimen that did not fracture in its central portion was not used.

A 24-h longitudinal tensile creep test was conducted with a load equivalent to 50% of the tensile strength. Applied stress is shown in Table 1. The load was removed immediately thereafter and maintained at 0 N until all strains became constant. Temperature (25°C) and humidity (55% RH) were kept constant during the test.

Decomposition of strain

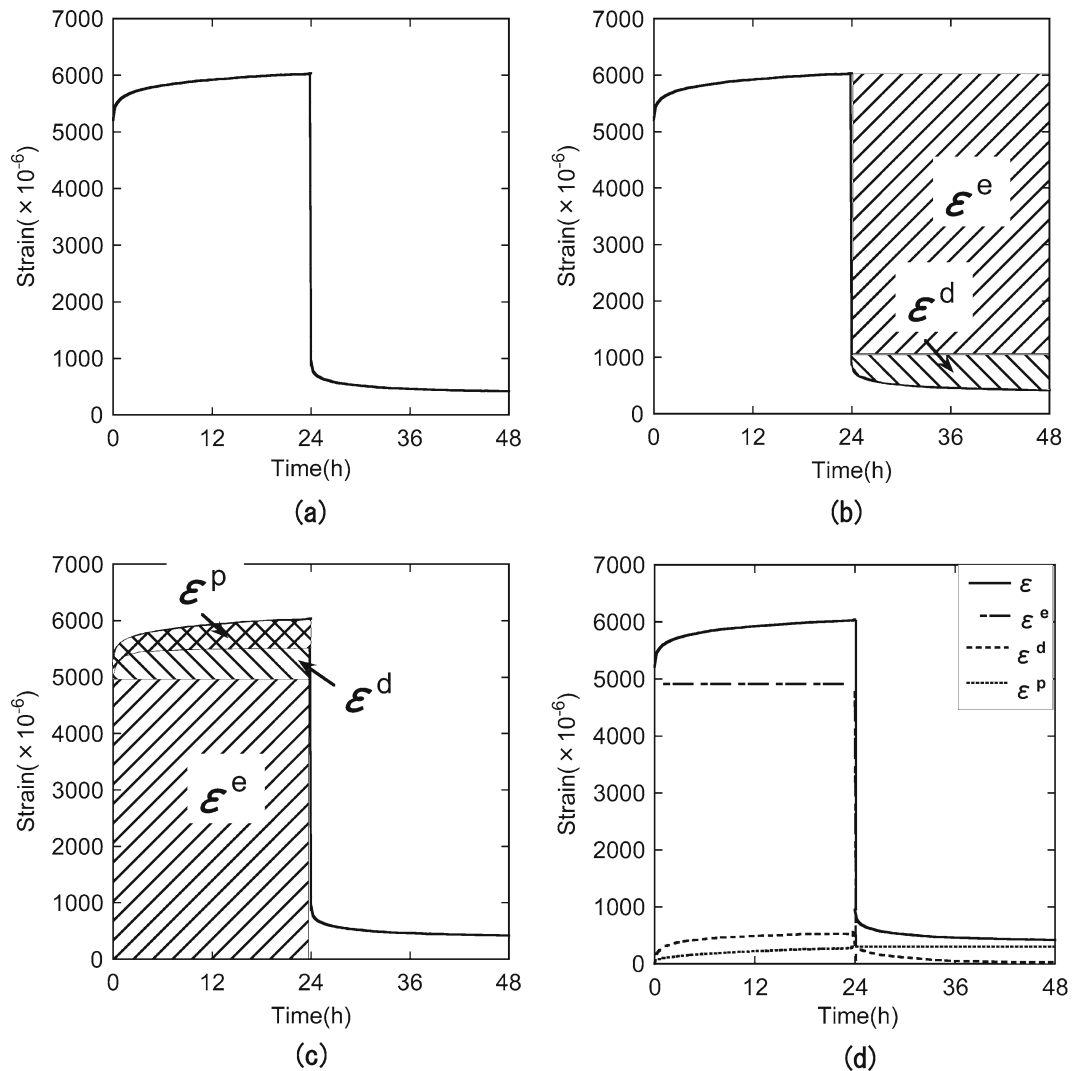
When a viscoelastic material such as wood is put under a time-dependent load condition, the resulting strain can be separated into the following three components: instantaneous strain (ϵ^e), delayed elastic strain (ϵ^d), and permanent strain (ϵ^p). Upon applying load, ϵ^e is generated at once, and upon removing the load, it returns to null at once. ϵ^d has time dependence. Upon applying a load, ϵ^d gradually increases with the elapse of time, and finally stabilizes at a certain value. Upon removal of the load, it gradually returns

to null. ϵ^p increases corresponding to the time of loading, but it never recovers after the removal of load. In this study, we attempted to separate the strain brought about by creep into instantaneous strain, delayed elastic strain, and permanent strain. The procedure for this compartmentalization is listed in Fig. 2:

1. The recovery strain just after the removal of load (when $dt/d\epsilon = 0$) is defined as instantaneous strain (ϵ^e ; Fig. 2b).
2. The value of the strain just before the removal of load after deducting ϵ^e and the entire strain at the recovery from creep is defined as delayed elastic strain (ϵ^d ; Fig. 2b).
3. It is assumed that the increased speed at creep in ϵ^d and the decreased speed at the recovery from creep in ϵ^d is the same. The time of the beginning of deformation in $\epsilon^e + \epsilon^d$ (shaded area in Fig. 2b) is shifted from 24 to 0 h (Fig. 2c). The value of the entire strain at creep after deducting $\epsilon^e + \epsilon^d$ is defined as the permanent strain (ϵ^p ; Fig. 2c).

An example of the longitudinal strain as separated out following this procedure is shown in Fig. 2d. The

Fig. 2. Procedure of the decomposition of longitudinal or lateral strain into three components at the creep and creep-recovery curve: **a** original curve; **b** step 1; **c** step 2; **d** decomposed strains at the curve. ϵ , entire strain; ϵ^e , instantaneous strain; ϵ^d , delayed elastic strain; ϵ^p , permanent strain



behavior of the permanent strain in this study was non-Newtonian.

Results and discussion

Changes in strain

Figure 3 shows the changes with time in the strains [longitudinal strain (ε_L) and lateral strains (ε_T , ε_R)] of Japanese cypress. Each strain is an average value on the opposite planes. The load was removed 24 h after the beginning of the creep test. The creep-recovery test was continued until all strains became constant. The lateral strain values are negative, but for the sake of convenience, they are shown as absolute values.

The changes in lateral strain were similar to those in longitudinal strain. That is, the absolute value of lateral strain continued to increase while the increase rate was gradually reduced during the creep; then, it recovered sharply just after the removal of the load, recovered slowly thereafter, and finally reached a constant value. We considered it possible to decompose the lateral strain into instantaneous strain, delayed elastic strain, and permanent strain, judging from the behavior observed during the recovery from creep.

Figure 4 shows the progression of the strain increase rate during creep in Japanese cypress. The rate of increase in the longitudinal strain during creep was continuously smaller than that in the absolute value of lateral strains.

Relationship between density and the strain increase rate

The density of wood is greatly dependent on its porosity. We examined the effects of the difference in porosity on the rate of increase in the strain. Figure 5 shows the relationship

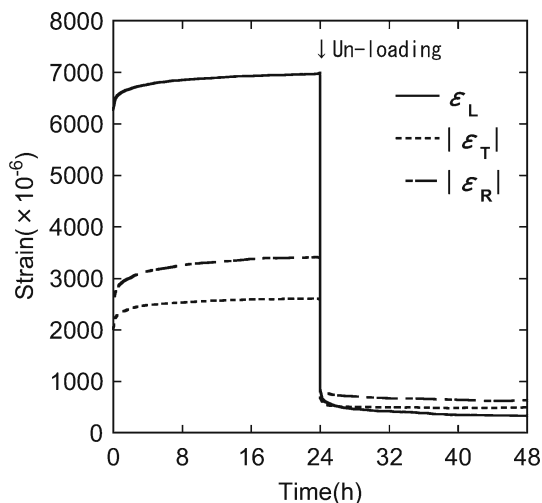


Fig. 3. Typical creep and creep-recovery curves in Japanese cypress. ε_L , longitudinal strain in a fiber direction; ε_T , lateral strain in a tangential direction; ε_R , lateral strain in a radial direction; ε_T and ε_R are represented by absolute values

between the strain increase rate after 24 h of creep and the density of 12 species. We cannot discuss here the species characteristics because the number of samples of each species is small; thus, we examined the relationship between density and Poisson's effect considering the wood as a homogeneous anisotropic material.

It is obvious that the rate of increase in ε_L is smaller than that in the absolute values of lateral strain (ε_T and ε_R). Also, there was not a significant difference between ε_T and ε_R (by t test). The rate of increase in ε_L had a negative relationship with density, although no relationship was observed in the ε_T and ε_R .

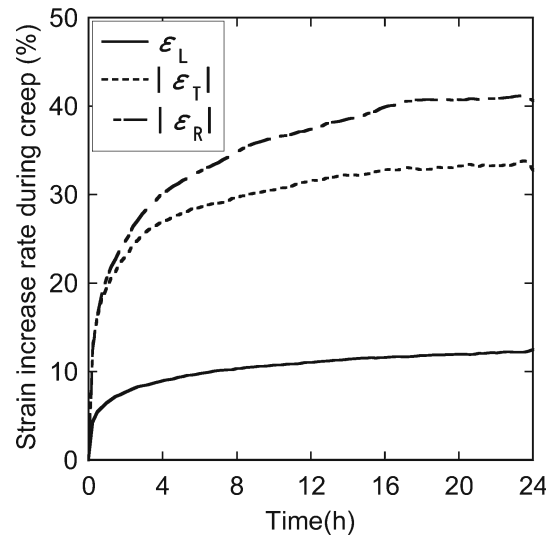


Fig. 4. Typical progression of the strain increase rate during creep in Japanese cypress. ε_T and ε_R are represented by absolute values

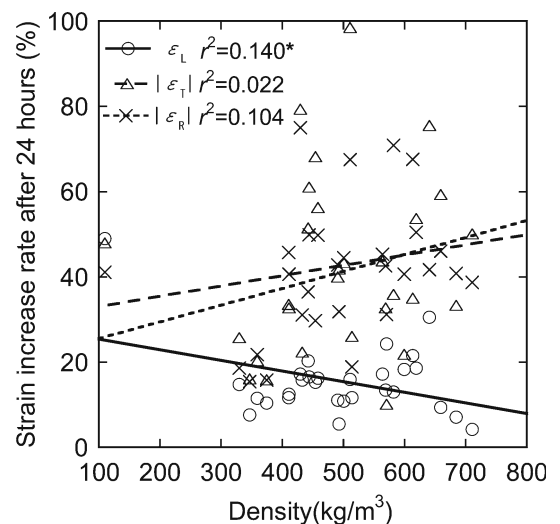


Fig. 5. Relationship between the rate of increase in the strain after 24 h of creep and the density of 12 species. ε_T and ε_R are represented by absolute values; ε_L , $y = -0.0250x + 27.9$; $|\varepsilon_T|$, $y = 0.0242x + 30.6$; $|\varepsilon_R|$, $y = 0.0396x + 21.6$. Asterisk, significant at 5% level

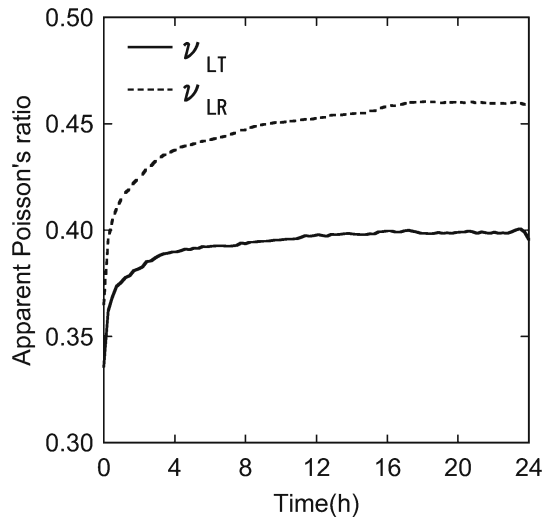


Fig. 6. Typical progression of apparent Poisson's ratio in Japanese cypress during the creep period

Changes in the apparent Poisson's ratio

Figure 6 shows the changes with time in the apparent Poisson's ratio during creep in Japanese cypress. Because Poisson's ratio is a constant based on the theory of elasticity, it does not change with time. In this study, the absolute value of the ratio of lateral strain to longitudinal strain was defined as the apparent Poisson's ratio to examine its behavior. The apparent Poisson's ratio can be expressed by the following equation:

$$\bar{\nu} = \left| \frac{\varepsilon_b}{\varepsilon_l} \right| \quad (2)$$

where ε_l is the longitudinal strain and ε_b is the lateral strain. It can be said that the larger the apparent Poisson's ratio, the larger the Poisson's effect.

At the initial stage of creep, both the apparent ν_{LR} and the apparent ν_{LT} increased sharply, because the increase in the absolute value of lateral strain was far greater than that in the longitudinal strain at the beginning of creep (see Fig. 4). Thereafter, both apparent ν_{LR} and apparent ν_{LT} gradually increased and finally reached virtually certain values.

Figure 7 shows the relationship between the rate of increase in the apparent Poisson's ratio after 24 h of creep and the density of 12 species. Only two values (ν_{LR} in balsa and ν_{LT} in Japanese beech) were negative. The increasing tendency of apparent Poisson's ratio in wood during creep is considered to be generally evident.

Relationship between density and apparent Poisson's ratio

Figure 8 shows the relationship between density and the apparent ν_{LR} immediately after the beginning of creep (ν_{LR0}) and after 24 h of creep (ν_{LR24}). Figure 9 shows the relationship between density and the apparent ν_{LT} immediately after the beginning of creep (ν_{LT0}) and after 24 h of creep (ν_{LT24}).

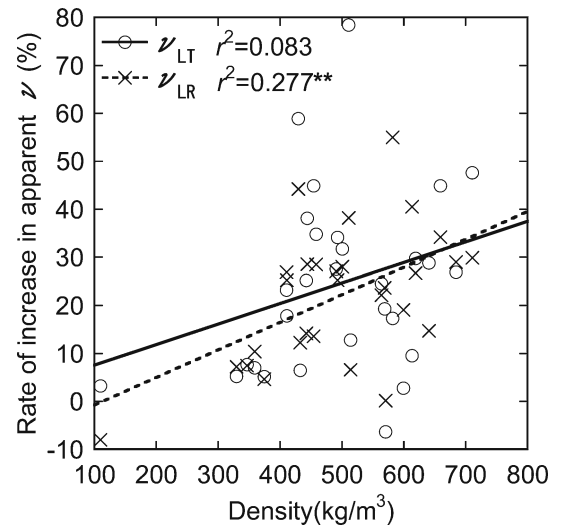


Fig. 7. Relationship between the rate of increase in apparent Poisson's ratio after 24 h of creep and density of 12 species. ν_{LT} , $y = 0.0428x + 3.28$; ν_{LR} , $y = 0.0575x - 6.49$. Double asterisk, significant at 1% level

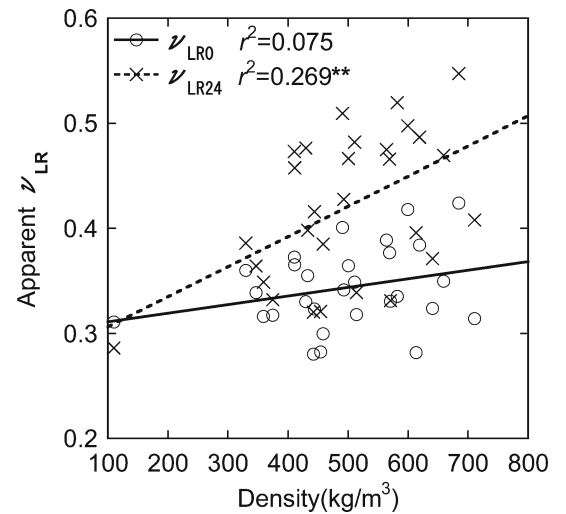


Fig. 8. Relationship between apparent Poisson's ratio (ν_{LR}) and density. ν_{LR0} , ν_{LR} at time = 0 h (just after loading); ν_{LR24} , ν_{LR} at time = 24 h (just before unloading); ν_{LR0} , $y = 0.0000822x + 0.303$; ν_{LR24} , $y = 0.000287x + 0.277$. Double asterisk, significant at 1% level

The characteristics common to both the apparent ν_{LR} (Fig. 8) and the apparent ν_{LT} (Fig. 9) are that both tended to increase with density, which is influenced by the porosity, and the gradient of the regression line was greater in the apparent Poisson's ratio after 24 h of creep.

Morooka et al.¹⁷ and Ohgama¹⁸ simulated the value of ν_{RT} for elastic bodies, considering the porous structure of wood, and showed a negative relationship with density. Yoshihara et al.²² also showed a negative relationship between density of compressed wood and ν_{RT} ; that is, their results were opposite to the tendency of the ν_{LR0} and ν_{LT0} in this study.

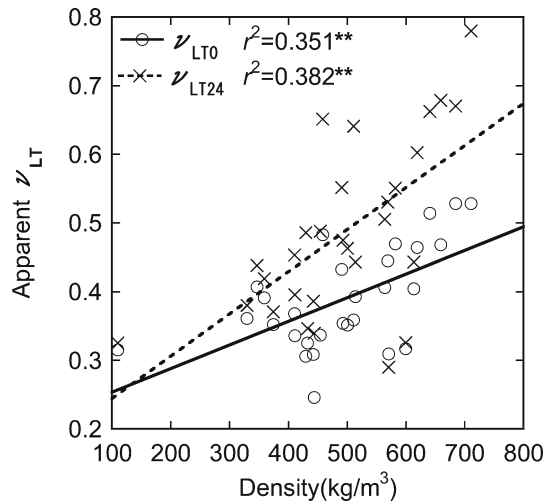


Fig. 9. Relationship between apparent Poisson's ratio (ν_{LT}) and density. ν_{LT0} , ν_{LT} at time = 0 h (just after loading); ν_{LT24} , ν_{LT} at time = 24 h (just before unloading); ν_{LT0} , $y = 0.000344x + 0.219$; ν_{LT24} , $y = 0.000613x + 0.183$. *Double asterisk*, significant at 1% level

Causes of the time dependence of Poisson's effect

Figure 6 shows that the apparent Poisson's ratio increases with time during creep. In the following paragraph, we examine the causes of this increase in the apparent Poisson's ratio. The lateral strain (ε_b) can be decomposed into the lateral instantaneous strain (ε_b^e), lateral delayed elastic strain (ε_b^d), and lateral permanent strain (ε_b^p) by following the procedure described above (see Fig. 2).

$$\varepsilon_b = \varepsilon_b^e + \varepsilon_b^d + \varepsilon_b^p \quad (3)$$

Equation 4 is obtained by substituting Eq. 3 for the right side in Eq. 2.

$$\bar{\nu} = \nu_e + \nu_d + \nu_p \quad (4)$$

$$\text{where } \nu_e = \left| \frac{\varepsilon_b^e}{\varepsilon_1} \right|, \quad \nu_d = \left| \frac{\varepsilon_b^d}{\varepsilon_1} \right|, \quad \nu_p = \left| \frac{\varepsilon_b^p}{\varepsilon_1} \right| \quad (5)$$

The apparent Poisson's ratio can be expressed as the sum of the three terms of the right side in Eq. 4, so it is possible to examine which strain component has the main effect on the apparent Poisson's ratio. These three terms (ν_e , ν_d , and ν_p) are designated as lateral-strain-determination coefficients. The lateral-strain-determination coefficients are the ratios of the lateral instantaneous strain, lateral delayed elastic strain, and lateral permanent strain to the entire longitudinal strain, respectively.

Figure 10 shows the changes in ν_d and ν_p at the apparent ν_{LR} in Japanese cypress, and Figure 11 shows the changes in ν_d and ν_p at the apparent ν_{LT} in Japanese cypress. For both ν_{LR} and ν_{LT} , the ν_d derived from the lateral delayed elastic strain becomes almost constant at the relative initial stage, whereas the ν_p derived from the lateral permanent strain continuously increases during creep. That is, it can be said that the Poisson's effect becomes greater with time as a result of the large contribution of the lateral permanent strain.

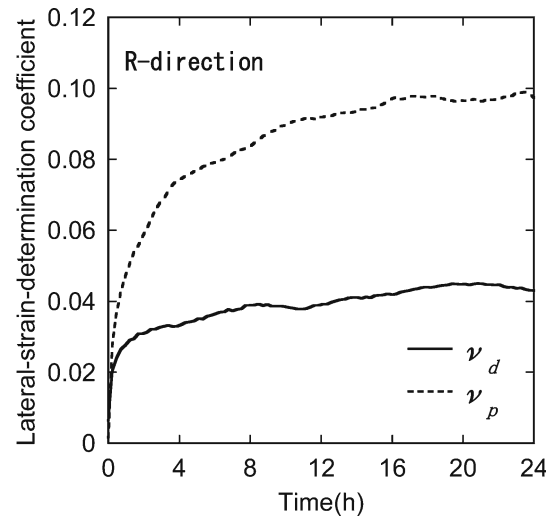


Fig. 10. Typical progression of lateral-strain-determination coefficient at apparent ν_{LR} in Japanese cypress during creep period. ν_d and ν_p are defined in Eq. 5

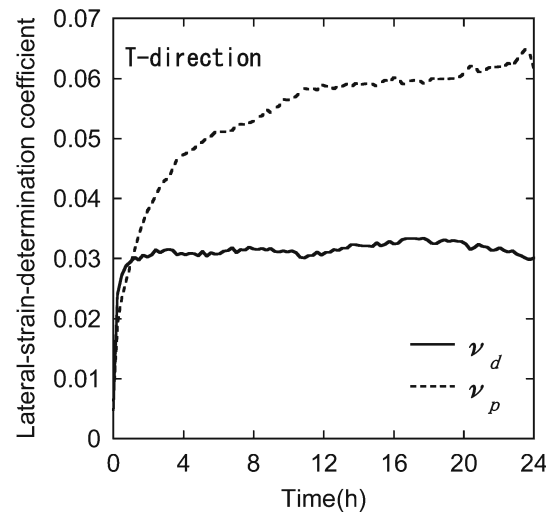


Fig. 11. Typical progression of lateral-strain-determination coefficient at apparent ν_{LT} in Japanese cypress during creep period. ν_d and ν_p are defined in Eq. 5

In some other materials [carbon fiber-reinforced plastics (CFRP)^{23,24}, glass fiber-reinforced plastics (GFRP)²⁴, and cortical bone²⁵], Poisson's ratio appeared to be more sensitive to microscopic damage development than the longitudinal Young's modulus. In this study, it is assumed that the lateral permanent strain is caused by the occurrence and expansion of microcracks in wood.

Conclusions

To understand the creep behavior of wood three dimensionally, a longitudinal tensile creep test for various species was conducted to examine the changes with time in the lateral strain and the apparent Poisson's ratio. The main results are listed below:

1. The changes in the lateral strain were similar to those in the longitudinal strain. That is, during creep, the absolute value of lateral strain continued to increase with the gradual reduction in the increase rate; immediately after the removal of the load, it recovered abruptly; then, it recovered slowly and finally reached a certain value.
2. The rate of increase in ε_L during creep was smaller than that in the absolute values of lateral strain (ε_T and ε_R).
3. At the initial stage of creep, the apparent Poisson's ratio rapidly increased. Then, it continued to increase gradually and finally reached a almost constant value. The apparent Poisson's ratio became large during creep because the lateral strain increased more than the longitudinal strain.
4. There was a positive correlation between apparent Poisson's ratio after 24 h of creep and density. On the other hand, there was a weak correlation between apparent Poisson's ratio immediately after the beginning of creep and density.
5. Analysis of lateral strain by separating it into three components, that is, instantaneous strain, delayed elastic strain, and permanent strain, has revealed that the lateral permanent strain in the transverse direction contributes most to the increase in the apparent Poisson's ratio during creep.

References

1. Navi P, Pittet V, Plummer CJG (2002) Transient moisture effects on wood creep. *Wood Sci Technol* 36:447–462
2. Kojima Y, Yamamoto H (2005) Effect of moisture content on the longitudinal tensile creep behavior of wood. *J Wood Sci* 51: 462–467
3. Hearmon RFS (1948) The elasticity of wood and plywood. Forest products research special report No. 7. His Majesty's Stationery Office, London
4. Yamai R (1957) On the orthotropic properties of wood in compression. *J Jpn For Soc* 39:328–338
5. Bodig J, Goodman JR (1973) Prediction of elastic parameters for wood. *Wood Sci* 5:249–264
6. Ljungdahl J, Berglund LA, Burman M (2006) Transverse anisotropy of compressive failure in European oak: a digital speckle photography study. *Holzforschung* 60:190–195
7. Keunecke D, Hering S, Niemz P (2008) Three-dimensional elastic behaviour of common yew and Norway spruce. *Wood Sci Technol* 42:633–647
8. Laghdir A, Fortin Y, De la Cruz CM, Hernández RE (2008) Development of a technique to determine the 3D elasticity tensor of wood as applied to drying stress modeling. *Maderas-Cienc Tecnol* 10:35–44
9. Niemz P, Caduff D (2008) Untersuchungen zur Bestimmung der Poissonschen Konstanten an Fichtenholz. *Holz Roh Werkst* 66: 1–4
10. Jeong GY, Zink-Sharp A, Hindman DP (2009) Tensile properties of earlywood and latewood from loblolly pine (*Pinus taeda*) using digital image correlation. *Wood Fiber Sci* 41:51–63
11. Yadama V, Wolcott MP (2006) Elastic properties of hot-pressed aspen strands. *Wood Fiber Sci* 38:742–750
12. Peura M, Grotkopp I, Lemke H, Vikkula A, Laine J, Müller M, Serimaa R (2006) Negative Poisson ratio of crystalline cellulose in kraft cooked Norway spruce. *Biomacromolecules* 7:1521–1528
13. Peura M, Kölln K, Grotkopp I, Saranpää P, Müller M, Serimaa R (2007) The effect of axial strain on crystalline cellulose in Norway spruce. *Wood Sci Technol* 41:565–583
14. Yoshihara H, Yamashita K (2004) Several examinations on the measurement methods for Poisson's ratio of wood (in Japanese). *Mokuzai Kogyo (Wood Industry)* 59:119–122
15. Bodig J, Jayne BA (1993) Mechanics of wood and wood composites. Krieger, Malabar
16. Carrington H (1922) The elastic constants of spruce as influenced by moisture. *Aëronaut J* 26:462–471
17. Morooka T, Ohgama T, Yamada T (1979) Poisson's ratio of porous material (in Japanese). *J Soc Mater Sci Jpn* 28:635–640
18. Ohgama T (1982) Poisson's ratio of wood as porous material (in Japanese). *Bull Fac Educ Chiba Univ Part II* 31:99–107
19. Hilton HH, Yi S (1998) The significance of (an)isotropic viscoelastic Poisson ratio stress and time dependencies. *Int J Solids Struct* 35:3081–3095
20. Hilton HH (2001) Implications and constraints of time-independent Poisson ratios in linear isotropic and anisotropic viscoelasticity. *J Elast* 63:221–251
21. Taniguchi Y, Ando K, Yamamoto H (2009) Determination of three-dimensional viscoelastic compliance in wood by tensile creep test. *J Wood Sci*. doi:10.1007/s10086-009-1069-6
22. Yoshihara H, Tsunematsu S (2007) Elastic properties of compressed spruce with respect to its cross section obtained under various compression ratios. *For Prod J* 57(4):98–100
23. Surgeon M, Vanswijgenhoven E, Wevers M, van der Biest O (1999) Transverse cracking and Poisson's ratio reduction in cross-ply carbon fibre-reinforced polymers. *J Mater Sci* 34:5513–5517
24. Kashtalyan M, Soutis C (2000) Stiffness degradation in cross-ply laminates damaged by transverse cracking and splitting. *Composites A* 31:335–351
25. Pidaparti RM, Vogt A (2002) Experimental investigation of Poisson's ratio as a damage parameter for bone fatigue. *J Biomed Mater Res* 59:282–287